

## Modeling fluvial erosion and deposition on continental shelves during sea level cycles

Sergio Fagherazzi

Department of Geological Sciences and School of Computational Science and Information Technology,  
Florida State University, Tallahassee, Florida, USA

Alan D. Howard and Patricia L. Wiberg

Department of Environmental Sciences, University of Virginia, Charlottesville, Virginia, USA

Received 8 September 2003; revised 23 April 2004; accepted 2 June 2004; published 18 August 2004.

[1] A numerical model has been developed to predict the evolution and degree of incision and deposition by fluvial channels on the continental shelf during sea level cycles. Rainfall-runoff, mass wasting processes, and fluvial sediment entrainment and transport are simulated using the detachment-limited model of *Howard* [1994] on a grid that represents the morphology of the continental shelf and corresponding coastal plain. The model is coupled with a deltaic module for sediment deposition in the ocean and a fluctuating sea level that mimics climatic changes on a  $\sim 10^4$  year timescale. The model indicates that the detailed structure of sea level oscillations has a strong influence upon sediment redistribution and channel development on the shelf. In particular, high-frequency sea level oscillations increase fluvial incision in the terminal reaches of the rivers due to rapid downcutting during the low stands of the oscillation. It is shown that the increment of incision at the river mouth is directly proportional to the oscillation amplitude. Furthermore, simulations indicate that an increase in river sediment load driven by climatic change favors channel avulsion with the formation of new fluvial incisions on the shelf. Results also show the strong influence of shelf morphology on establishing channel networks during sea level low stands. *INDEX TERMS*: 1625 Global Change:

Geomorphology and weathering (1824, 1886); 1815 Hydrology: Erosion and sedimentation; 1824 Hydrology: Geomorphology (1625); 3210 Mathematical Geophysics: Modeling; 4219 Oceanography: General: Continental shelf processes; *KEYWORDS*: fluvial incision, continental shelf, sea level cycles

**Citation:** Fagherazzi, S., A. D. Howard, and P. L. Wiberg (2004), Modeling fluvial erosion and deposition on continental shelves during sea level cycles, *J. Geophys. Res.*, 109, F03010, doi:10.1029/2003JF000091.

### 1. Introduction

[2] During sea level low stands, broad areas of the continental shelf are exposed to rainfall-runoff, allowing a fluvial channel network to develop with related incised valleys. During subsequent transgressions, fluvial and estuarine deposition as well as sediment reworking by waves and currents fills and partly erases the river network, leading to a system of buried channels beneath the continental shelf surface [*Dalrymple et al.*, 1994].

[3] The presence of buried channels and related paleovalleys is well documented for the major rivers flowing into the Atlantic and Gulf of Mexico coasts. Seismic reflection profiles indicate that during the last Pleistocene glaciation the Delaware River flowed across the continental shelf and emptied into Wilmington canyon, east of Delaware Bay, with a paleovalley 3–8 km wide and a channel base 10–30 m deeper than the adjacent terraces [*Twichell et al.*, 1977]. Six fluvial erosion surfaces with paleovalleys up to 5

km wide and 35 m deep caused by high-frequency Quaternary sea level oscillations are preserved in the sediments beneath the Virginia inner shelf [*Foyle and Oertel*, 1997]. Analyses of seismic reflection profiles collected off New Jersey reveal a large paleovalley, probably the ancestral pathway of the Hudson River, with a width of 2–17 km and relief of 3–15 m [*Knebel et al.*, 1979].

[4] It is likely that during sea level low stands a riverine network, similar to the channels that dissect the present coastal plain, occupied the entire area of exposed shelf. As a consequence, a dendritic system of buried paleochannels (with dimensions ranging from hundreds to tens of meters in width) is preserved in the geological record in some shelf locations, as, for example, in front of Chesapeake Bay [*Chen et al.*, 1995] or in the middle of the New Jersey continental shelf [*Duncan et al.*, 2000].

[5] The stratigraphy of the middle New Jersey continental shelf reflects the pulsed episodicity of the last sea level cycle [*Duncan et al.*, 2000]. The intermittent advance of ice sheets during the latest Pleistocene regressions and transgressions ( $\sim 120$ –25 ka) and corresponding fluctuations of the shoreline produced several regressive and transgressive

ravinement surfaces and an outer shelf wedge. Seismic data show that a regressive surface 45 kyr old was truncated by a second erosion surface, characterized by the presence of numerous paleochannels, that was interpreted as a long period of fluvial incision related to the Wisconsin glacial maximum ( $\sim 25\text{--}15$  ka), when the shelf was subaerially exposed. During the subsequent early Holocene transgression ( $\sim 15\text{--}10$  ka), incised channels were filled with a succession of lagoonal and estuarine muds. The most recent part of the transgression ( $\sim 10\text{--}0$  ka) then erased all bathymetric evidence of features older than 16 ka through the reworking of the sediments by shelf processes. A map of paleochannels created from interpretations of the seismic profiles shows dendritic valleys (typically  $>10$  m deep and hundreds of meters long) feeding into larger channels, oriented northwest-southeast. This dendritic network extends through essentially all the surveyed area [Davies and Austin, 1997].

[6] Few studies have quantitatively addressed the creation and development of river networks on the continental shelf during sea level low stands or their potential burial or erasure during subsequent sea level transgression. A recently proposed numerical model investigates the quantitative behavior of river shelf sedimentary systems under glacioeustatic conditions [Meijer, 2002]. The model favors the formation of a diffuse channel system, with several deltaic distributaries, on the shelf during sea level fall. When the shoreline drops below the shelf edge, headward erosion and knickpoint retreat concentrates the discharge and sediment load in a single channel, connecting the drainage basin to the depositor on the shelf edge, thereby bypassing the exposed shelf. We argue that a diffuse channel system is only present in the deltaic area, whose extension is limited in comparison to the shelf width. In our viewpoint the transport of sediment to the ocean is always concentrated in few rivers dissecting the shelf, and only at large timescales (hundreds of thousands of years) can we view the redistribution of the sediments on the shelf as a diffusive process during low stands [Paola et al., 1992; Marr et al., 2000]. Furthermore, Meijer's [2002] model only focuses on the evolution of a single fluvial system, without exploring the combined behavior of both local drainage and that from channels from continental drainage systems debauching onto the shelf.

[7] The fluvial response to sea level changes has also been studied through experiments [van Heijst and Postma, 2001; van Heijst et al., 2001; Wood et al., 1993]. These experiments show that neither fall nor rise in sea level affects the fluvial system instantaneously and that river profile adjustment occurs through migration of knickpoints with a time lag between sea level fall and the upstream adjustment of the river's longitudinal profile. However, the physical constraints and the highly distorted scales of the experiments often favor sheet flow rather than concentrating the water discharge in localized streams, thus increasing the spatial diffusion of the sediments and failing to capture the concentration of deposits in localized shelf areas.

[8] In this paper we present a numerical model to predict the nature and the degree of incision of fluvial channels on the continental shelf during periods of sea level variation. The model is able, via a simplified approach, to address fluvial response (in terms of valley evolution) to sea level changes and, most importantly, to keep account of the three-

dimensional structure of the shelf and channel network. We then utilize the model to (1) analyze the response of the fluvial-shelf system to both high-frequency (centennial scale) and low-frequency (millennial scale) sea level oscillations; (2) assess the influence of changes in sediment load and river discharge driven by climatic variations on the shelf channels; and (3) determine the influence of the shelf topography on the establishing fluvial networks.

[9] We begin by reviewing some of the important controls on channelization of exposed continental shelves. We next describe the model and then present and discuss a series of exploratory simulations designed to investigate the effects of these controls on channel incision and river network development.

## 2. Controls on Channel Development on the Shelf

[10] The coevolution of landscapes and fluvial networks is one of the most intriguing and complex topics of geomorphology. Among the factors that govern the formation and evolution of riverine channels on the continental shelf are (1) the river response to base-level changes; (2) the shape and volume of alluvial deposits; (3) the geometry and slope of the shelf relative to the coastal plain and shoreface; (4) the position of minimum sea level relative to the shelf edge; (5) the frequency and magnitude of sea level oscillations; and (6) the discharge and sediment load of the incoming rivers.

[11] River responses to base-level rise or lowering have been reported in different, and sometimes contradictory, ways (see Blum and Törnqvist [2000] for a review). Leopold and Bull [1979] observed that upstream effects of sea level rise are limited in modern rivers. On the other hand, Fisk [1944] reported that the drop in sea level during the last glaciation produced deep incision in the Mississippi Valley 1000 km upstream from the present shoreline. At the same time, Schumm [1993] pointed out that a change in base level can be reflected not only in a variation of stream gradient but also in an adjustment of channel pattern, roughness, and shape. He concluded that the upstream effects of base-level change are moderated and will happen mostly through a change in sinuosity and channel dimensions. However, despite different opinions among researchers, it is reasonable to assume that a river may partly adjust its shape and pattern to counteract base level changes but that it will also readjust its gradient through incision and aggradation.

[12] Recent studies of sea level history, based on high-resolution oxygen isotope records, seem to suggest that sea level change during the last glacial cycle occurred at rates of up to  $2\text{ cm yr}^{-1}$  over an elevation range of 35 m [Siddall et al., 2003]. The fluvial-shelf system probably felt the effects of these high-frequency oscillations in base level, both in terms of fluvial incision and development of deltaic deposits. Total channel incision and the geometry of the deltaic deposits are thus sensitive to the ratio between the response time of the fluvial-shelf system and the timescale of the sea level oscillations.

[13] Channel incision during low stands is affected by the shape and location of deltaic deposits. Talling [1998] recognized the importance of high-stand deposit thickness (i.e., the coastal prism) on the subsequent incision of the continental shelf. He assumed that if sea level does not fall below the shelf slope break, the major valley incision will

occur where convex coastal prisms are deposited during high stands.

[14] The three-dimensional shape of the coastal plain–continental shelf system is also of fundamental importance for the development of the river network as well as for the redistribution of alluvial sediment through erosion and deposition. For example, the concept of accommodation (i.e., the space available below base level for the sediment to accumulate [Jervy, 1988]) has to be extended to the three-dimensional structure of the shelf. Channel extension and incision during sea level fall are also influenced by geometrical differences between the coastal plain and shelf. Summerfield [1985] suggested that a coastal plain slope smaller than the shelf slope leads to channel extension with deep incision during sea level fall, while a coastal plain slope greater than the shelf slope produces channel extension with progradation and aggradation.

[15] When sea level drops below the shelf slope break, deep channel incision and knickpoint retreat are initiated. The migration of knickpoints along the river implies a time lag between sea level low stands and the upstream adjustment of the river's longitudinal profile [Butcher, 1990]. The magnitude of this time lag is still under discussion [Shanley and McCabe, 1994] but again depends on the ratio between the characteristic temporal scales of river profile adjustment and sea level oscillations.

[16] Finally, changes in river flood regimes and sediment loads associated with climate change strongly influence sedimentary processes on shelves and coastal plains [Blum and Törnqvist, 2000; Leeder et al., 1998; Perlmutter and Matthews, 1989; Perlmutter et al., 1998]. Such changes may include sediment yield and flood frequency and magnitude [Knox, 1993; Probst, 1989; Syvitski et al., 2003], vegetation cover [Knox, 1983; Langbein and Schumm, 1958], and glacial effects on sediment production and discharge [Hallet et al., 1996].

### 3. Drainage Basin Model

[17] Several geomorphic processes are likely to have occurred on emergent continental shelves during sea level low stands: weathering of exposed sediments by chemical and physical agents, erosion by running water (with a source from runoff and with contributions from groundwater seepage), creep, threshold mass wasting, and landsliding. Sediment transport and deposition act together to shape the continental shelf landscape and to carve a network of fluvial channels. We simulate most of these processes utilizing the detachment-limited model (DELIM) of Howard [1994, 1997]. The principal components of the model are briefly described and discussed in the context of continental shelf erosion.

#### 3.1. Weathering

[18] In the model described by Howard [1994] the vertical structure of the landscape is divided into two layers, regolith and bedrock. This distinction reflects the inherent difference in mechanical properties, with the bedrock more resistant to erosion. During landscape evolution, part of the bedrock is transformed into regolith due to weathering processes. Because of the intrinsically weak nature and high erodibility of continental shelf sediments [e.g., Howard and

Kerby, 1983], we assume that reduction in erosive properties by weathering are inconsequential.

#### 3.2. Mass Wasting

[19] Diffusive mass wasting due to soil creep, biogenic activity, rain splash, and runoff can be represented by a diffusion equation. At each point of the landscape the diffusive character of mass wasting processes is captured by the following equation:

$$\frac{\partial z}{\partial t} = K_S \left( \frac{\partial^2 z}{\partial x^2} + \frac{\partial^2 z}{\partial y^2} \right), \quad (1)$$

where  $z$  is the surface elevation,  $K_S$  is the creep diffusivity,  $t$  is time, and  $x$  and  $y$  are the spatial coordinates.

[20] Equation (1) is based on mass conservation and on the hypothesis that the sediment flux is linearly proportional to the topographic slope. In steep, mantled landscapes the sediment flux most likely increases for slopes near the failure slope, and equation (1) should be modified to account for this nonlinear mechanism [Howard, 1994; Roering et al., 1999]. However, the gentle slopes of continental shelves and coastal plains suggest that near-failure mass wasting (debris flow and landsliding) is a negligible process and that equation (1) is sufficient to describe mass wasting processes. For humid, temperate, and vegetated terrain,  $K_S$  might vary between 0.0001 and 0.001 m<sup>2</sup> yr<sup>-1</sup>. For example, Carson and Kirkby [1972, p. 288] reported a value of 0.00013 m<sup>2</sup> yr<sup>-1</sup> for coastal plains near Baltimore, Maryland. In the model we implemented diffusive mass wasting with an explicit finite difference formulation. At each time step the elevation of every node is updated as a function of the neighboring elevations following equation (1).

#### 3.3. Rainfall and Drainage Area

[21] The fluvial network that routes rainfall to the ocean is the dominant mechanism for erosion and deposition of coastal plain sediments. Fluvial discharge is directly linked to drainage area so that the latter is used as a surrogate variable. In the model, each square element of the computational grid drains into one of the eight neighboring elements following the steepest descent direction; we then calculate the drainage area as the sum of the areas of the elements that are connected upstream to the considered point. River avulsion occurs only if sediment deposition increases the elevation of the downstream cell so that the steepest descent direction changes, obliging the flow of water and sediments to follow a different route to the ocean. In our model, avulsion occurs whenever such a change occurs, without a threshold criterion such as suggested by Sun et al. [2002] and Mohrig et al. [2000].

[22] This implementation differs from the one proposed by Meijer [2002] in his coupled fluvial-shelf model. In Meijer's [2002] model, water and sediments can leave each cell in different directions, provided that the downslope grid cells have lower elevation, with a slope higher than a specific threshold. This implementation favors diffusive transport and river avulsion not only in the delta area but also in the coastal plain and in the piedmont. However, downstream branching of rivers generally occurs only in deltaic and fan environments. In our model, distributaries occur implicitly on aggrading fluvial surfaces through



frequent channel avulsions. Within incised valleys, flows are constrained except for, possibly, local braiding, which cannot be represented in these coarse-grained models.

[23] Particular attention has to be given to the treatment of depressions (pits) when fluvial routing is applied to the continental shelf. In fact, contrary to nonglacial coastal plains, where few lakes are present, broad, shallow depressions are found on the continental shelf. These depressions appear to be associated with construction of large offshore sand ridges and relict topographic features. In the model, depressions are assumed to be filled with water. Discharge that enters the depression exits at the lowest boundary point without loss, following the procedure delineated by *Jenson and Domingue* [1988]. The sediment entering a depression is accumulated in a deltaic deposit, and no sediment is transported through the depression until it is filled. We do not simulate bottomset suspended load beds.

### 3.4. Detachment-Limited Fluvial Erosion

[24] Once the drainage area pertaining to each channel is determined, the amount of sediment eroded or deposited at each location is calculated. In headward channel tracts, bed load sediment flux can be less than the capacity load of the stream. In this situation the amount of sediment transported by the river depends on the ability to entrain material from the regolith or bedrock bottom (detachment-limited erosion). The detachment capacity is assumed to be proportional to the shear stress that the flow exerts on the bed. The erosion rate can then be expressed as

$$\begin{aligned} \frac{\partial z}{\partial t} &= -K_T(\tau - \tau_c) & \tau &\geq \tau_c \\ \frac{\partial z}{\partial t} &= 0 & \tau &< \tau_c, \end{aligned} \quad (2)$$

where  $\tau$  is the shear stress,  $\tau_c$  is the critical shear stress for entrainment, and  $K_T$  is a constant of proportionality. Assuming steady, uniform flow and consistent downstream hydraulic geometry, we can link shear stress to drainage area and bed slope [*Howard*, 1994] (see Appendix A). Equation (2) then becomes

$$\frac{\partial z}{\partial t} = -K_T \left( K_Z A^{0.6e(1-b)} S^{0.7} - \tau_c \right), \quad (3)$$

where  $b$  is the width exponent of the hydraulic geometry and  $e$  is the exponent relating discharge to drainage area (see Appendix A). Here we use the downstream hydraulic geometry parameters for Appalachian streams calculated by *Brush* [1961]. Furthermore, 10 years of measurements of channel erosion in an unvegetated borrow pit in Virginia coastal plain sediments [*Howard and Kerby*, 1983] allowed us to calibrate the parameters  $K_T$  and  $K_Z$  (yielding  $K_T = 0.015 \text{ m}^3 (\text{N yr})^{-1}$  and  $K_Z = 932.0 \text{ kg m}^{-1.422} \text{ s}^2$ ). The critical shear stress  $\tau_c$  ranges from 10–40  $\text{N m}^{-2}$  for bare upland soils to 300–3000  $\text{N m}^{-2}$  for forested soils, reflecting the importance of vegetation in increasing the soil resistance to erosion. Critical shear stress for unconsolidated shelf sediment is likely to be even lower than these values, and we assume that the critical shear stress is negligible.

[25] A list of the parameter values adopted in the simulations is reported in Table 1. The derivation of these values is fully described in Appendix A. Once the sediment is

**Table 1.** Model Parameters

Parameter	Value
$K_S, \text{m}^2 \text{yr}^{-1}$	0.00013 <sup>a</sup>
$e$	0.8 <sup>b</sup>
$b$	0.56 <sup>b</sup>
$a$	0.39 <sup>b</sup>
$c$	0.053 <sup>b</sup>
$K_{D1}, \text{s}^{0.56} \text{m}^{-0.68}$	2.02 <sup>b</sup>
$K_{D2}, \text{s}^{0.39} \text{m}^{-0.17}$	0.60 <sup>b</sup>
$K_{D3}, \text{s}^{0.053} \text{m}^{-0.84}$	0.8 <sup>b</sup>
$K_T, \text{m}^3 (\text{N yr})^{-1}$	0.015 <sup>c</sup>
$K_Z, \text{kg m}^{-1.422} \text{s}^2$	932.0 <sup>c</sup>
$K_q, \text{m}^{2.104} \text{yr}^{-1}$	15.0
$K_v, \text{m}^{-0.422}$	288.0

<sup>a</sup>From *Carson and Kirkby* [1972].

<sup>b</sup>From *Brush* [1961].

<sup>c</sup>From *Howard and Kerby* [1983].

detached, it is instantaneously routed through the channel until the river becomes transport limited.

### 3.5. Transport-Limited Fluvial Erosion and Deposition

[26] When the bed load sediment flux is equal to the stream capacity, the river is said to be transport limited. In this case, changes in channel elevation depend on the divergence of the sediment discharge:

$$\frac{\partial z}{\partial t} = \frac{1}{\alpha} (Q_{sb}^{\text{in}} - Q_{sb}^{\text{out}}), \quad (4)$$

where  $Q_{sb}$  is the volumetric sediment discharge entering or leaving a grid element and  $\alpha$  is the element area. The sediment discharge can be calculated using steady state formulations and expressed in terms of drainage area and bottom slope (as for the detachment-limited case). For example, using the Einstein-Brown equation for total sediment load, we derive the following expression:

$$Q_{sb} = K_q A^{eb} \left( K_v A^{0.6e(1-b)} S^{0.7} \right)^3, \quad (5)$$

where  $K_q$  and  $K_v$  are suitable parameters. Calibration of the equations for piedmont landscapes in the northeast United States leads to the values reported in Table 1 (see Appendix A). In the model we track the thickness of alluvium in each cell, and we use equation (5) (transport-limited erosion and deposition) only when this thickness is greater than zero; otherwise, we use equation (2) (detachment-limited erosion). Transitions from detachment-limited to transport-limited conditions occur when actual channel gradients drop to values lower than that given by solving equation (5) for the equilibrium alluvial channel gradient.

[27] Solutions to equation (4) are prone to numerical instabilities when implemented along a river profile [*Fagherazzi et al.*, 2002]. To circumvent this numerical problem, we utilize the algorithm presented by *Howard* [1994] which updates the channel gradient based on the equilibrium river slope calculated from equation (5) once the sediment load and the discharge are computed in each river node (for details, see *Howard* [1994]).

[28] Sediment is routed at the equilibrium gradient with deposition or erosion along the length of the alluvial channel in accord with mass conservation of bed sediment

supplied from upstream. The fraction of total load supplied from upstream erosion that is bed load is set as a simulation parameter; we set the value at 10%. We assume that transport of suspended and wash load occurs without deposition within the fluvial system, and we do not track offshore sedimentation of wash load in these simulations. Since the model is determining the average elevation of the river bottom over a large distance, the fluvial incision calculated by the model corresponds to the “fluvial incision” defined by *Salter* [1993] and not to the “fluvial scour” that depends on local bottom variations within a channel reach [*Salter*, 1993; *Best and Ashworth*, 1997].

### 3.6. Deltaic Deposition and Coastal Processes

[29] Once alluvial sediments reach the ocean, they are deposited in deltas and estuaries. In the deltaic module the foreset slope is provided as an input parameter, whereas the terminal topset slope is set equal to the equilibrium slope (at grade), derived by equation (5) from the given drainage area and sediment discharge. Sediments are deposited at the delta foreset, maintaining constant topset and foreset slopes. Thus the geometric characteristics of the delta are set a priori, but the rate of deposition at the delta margin and the total delta volume are controlled by sediment supply from upstream.

[30] The reworking of sediments by currents and waves in the shallow areas of the shelf would be expected to change the location of sediment deposits, modifying the morphology of the shelf. The new morphology, during regression, would then influence the pattern of the establishing rivers. In these preliminary simulations we do not consider the influence of coastal processes on shelf topography. This idealized schematization without waves and currents corresponds to fluvial-dominated coastlines (as compared to wave- or tide-dominated coastlines). We focus on fluvial processes and the consequences of base-level changes in their evolution. The present formulation can be utilized as a benchmark for comparisons when coastal processes are also taken into account.

### 3.7. Implementation and Model Constraints

[31] In the present model the channel dimensions are not explicitly calculated but are embedded in the hydraulic geometry relationships (see Appendix A). As a consequence, the series of square cells that define the topography represent the valley form but do not represent the details of channel pattern. Processes that form meanders are not taken into account so that the river is unable to widen its valley through bend migration. Consequently, changes in river sinuosity and geometry [see *Schumm*, 1993] are not included, and the only adjustment to the river allowed in the model is in bottom slope. Lateral channel migration and valley widening have a strong influence on the development of fluvial patterns on the shelf but probably do not consistently modify the quantity of sediment delivered to the coast in the long term. However, through sediment storage in river bars and terraces, lateral channel migration can delay or accelerate sediment delivery, perhaps leading to a complex nonlinear response of the fluvial-shelf system.

[32] A no flux boundary condition for both water and sediments is implemented at the lateral and upper edges of the computational domain, while at the bottom edge we

allow an outgoing flux. However, at the upper edge we can specify the discharge and the sediment load of incoming rivers. Since the no flux boundary conditions at the lateral edges can locally influence channel development, particular attention must be devoted to the interpretation of the model results near the boundaries. We do not include subsidence in our model, so eustatic sea level is equivalent to relative sea level in our simulations.

## 4. Simulations

[33] In the simulations the continental shelf and the upper part of the continental slope are idealized as two flat, tilted planes intersecting each other (Figure 1a). The slope of the continental shelf ( $\sim 0.0008$ ) and its width ( $\sim 100$  km) are similar to those of the Atlantic shelf offshore of Virginia. We consider only the upper part of the continental slope, to a depth of 180 m (Figure 1a); the slope below the shelf break is set to 0.004. At the top edge of the simulation domain an incoming river having a drainage area of the same magnitude of the modern Delaware river is considered (drainage area =  $0.017 \cdot 10^6$  km<sup>2</sup> [from *Milliman and Syvitski*, 1992]), with a total sediment load  $Q_{sb} = 800,000$  m<sup>3</sup> yr<sup>-1</sup>. Each element of the mesh is  $1000 \times 1000$  m, and the time step is  $\sim 10$  years but varies depending on the incision rate for numerical stability. The size of the domain is different in each simulation.

### 4.1. Effect of Varying Sea Level

[34] Analysis of sea level oscillations in the recent past clearly shows that elevation changes of the order of tens of meters occur in a time span of thousands of years (see Figure 1d, derived from *Chappell et al.* [1996]). To investigate the role of intermediate sea levels in the development of drainage patterns and incision, we utilize the sea level history near the end of the Wisconsin glaciation (interval A–C in Figure 1d).

[35] In the first simulation we added a random elevation uniformly distributed between  $-5$  and  $5$  m to the initial topography to simulate the local asperities of the shelf. The size of the domain is  $80 \times 270$  km.

[36] The relatively rapid drop in sea level moves the delta foreset seaward (Figures 1a and 1b). Given the widespread sediment deposition and the absence of topographic asperities, there are not particular areas prone to channel incision for the incoming large river until the sea level drops below the continental shelf edge (Figures 1b and 1c). At this point the river regrades, cutting sediment deposits through a migrating knickpoint (Figures 1e and 1f).

[37] When sea level drops below the continental shelf break, fluvial incision involves both downcutting on the low gradient upper shelf and headward migration of knickpoints originating at the shelf break. Because the intrinsic erodibility of coastal plain sediments is high (we assume  $K_T = 0.015$  m<sup>3</sup> (N yr)<sup>-1</sup> based upon measurements by *Howard and Kerby* [1983]), predicted incision rates are very high, e.g.,  $\sim 0.1$  m yr<sup>-1</sup> for the trunk channel of a local drainage basin on the shelf with a 900 km<sup>2</sup> drainage area, an effective discharge of 250 m<sup>3</sup> s<sup>-1</sup>, and a gradient of 0.0008.

[38] In the simulations and, we presume, in Quaternary drainage channels incised into the shelf the larger channels become transport limited, except at their headwater tips. The

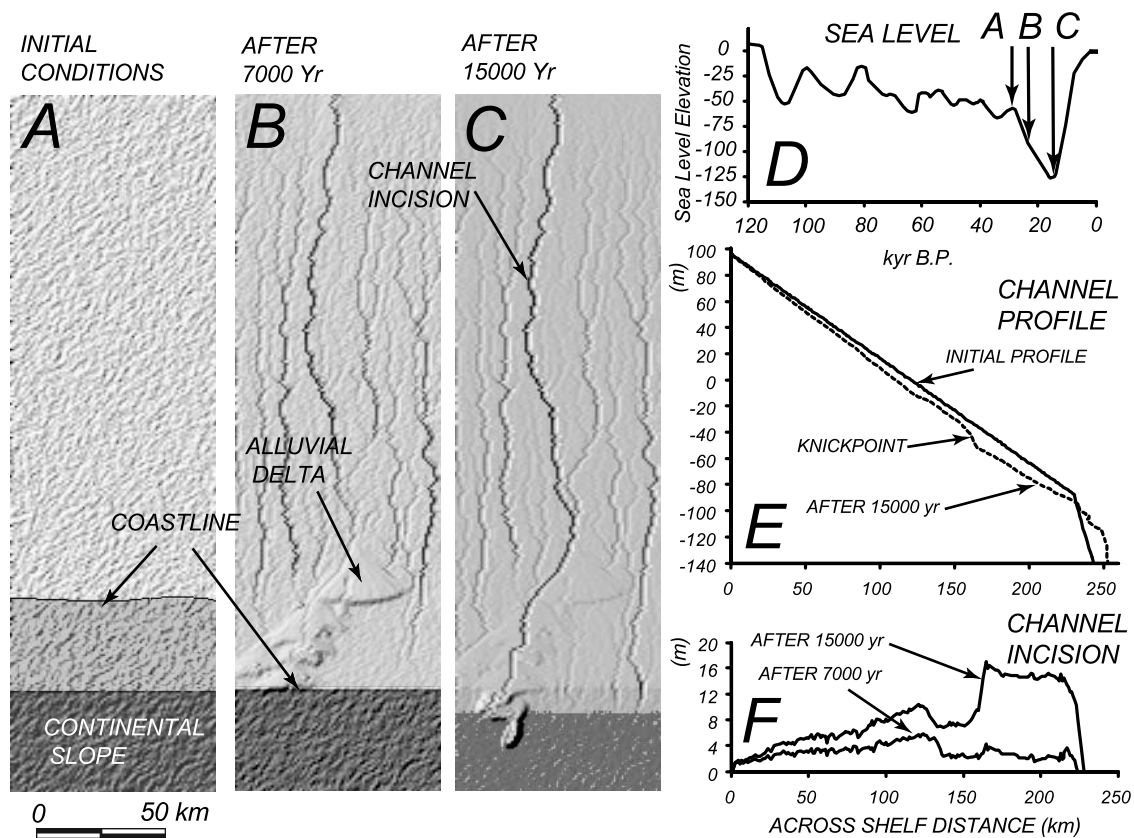


**Figure 1.** Establishment of fluvial channels on the continental shelf after sea level fall. A river flows in the middle of the simulation domain. (a) Initial conditions. (b) After 7000 years. A complex series of deltaic deposits form on the shelf. The relatively rapid decrease in sea level produces a continuous depositional system, with low channel incision. (c) After 15,000 years. The sea level is below the shelf edge, leading to consistent incision along the river profile. (d) Sea level oscillations in the last 120 kyr [adapted from *Chappell et al.*, 1996]. The interval from A to C is utilized in the simulations to study the influence of real sea level fluctuations on the establishment of fluvial channels in the shelf. (e) Channel profile. (f) Channel incision. The gray scale in Figures 1a–1c is proportional to the local topographic slope.

exceptions are local knickpoints that develop and migrate rapidly headward where steeper slopes are exposed on the shelf during sea level fall. These local knickpoints generally diminish in height during headward erosion and dissipate rapidly, being replaced by transport-limited channels. Larger knickpoints are generated as sea level falls below the shelf break. These knickpoints erode headward for the  $\sim 10,000$  years that sea level remains below the break. For larger local drainages in the simulations, simulated knickpoints in exposed coastal plain sediments roughly 10 m high progressed 60 km headward from the shelf break. Above and below, the knickpoint channels are transport limited.

[39] In the simulation, several channels become established on the shelf next to the major channel (Figure 1c). The watersheds of these channels are entirely included within the shelf, and the sediments transported in them have a local origin. In simulations such as this, where the

shelf is modeled as a flat plane, the minor channels are almost parallel and seldom discharge into the principal river under study (Figure 1c). Local channels spontaneously form as a result of rainfall-runoff when the discharge exceeds the threshold value for erosion.

[40] Two important consequences are associated with a rapid rate of sea level fall. First, it is difficult to separate the high stand river deposits from the low stand deposits. Rather, a continuous and asymmetric depositional system forms with variable thickness. Second, the river pattern is strongly influenced, through avulsion, by the alluvial deposits. For a river at grade on the shelf and sea level that does not fall below the slope, channel incision is negligible (Figure 1b). Significant incision only develops when sea level falls below the continental slope break.

[41] A simulation with identical initial and boundary conditions but considering the full sea level oscillations

**Figure 2.** Simulation of fluvial incision and related deltaic deposits utilizing sea level oscillations for the last 120 kyr. Simulation parameters and shelf geometry are identical to the simulation of Figure 1. (a–i) Model results at different time steps and for different sea level elevations. (j) Sea level curve indicating the sea level elevations corresponding to the Figures 2a–2i.



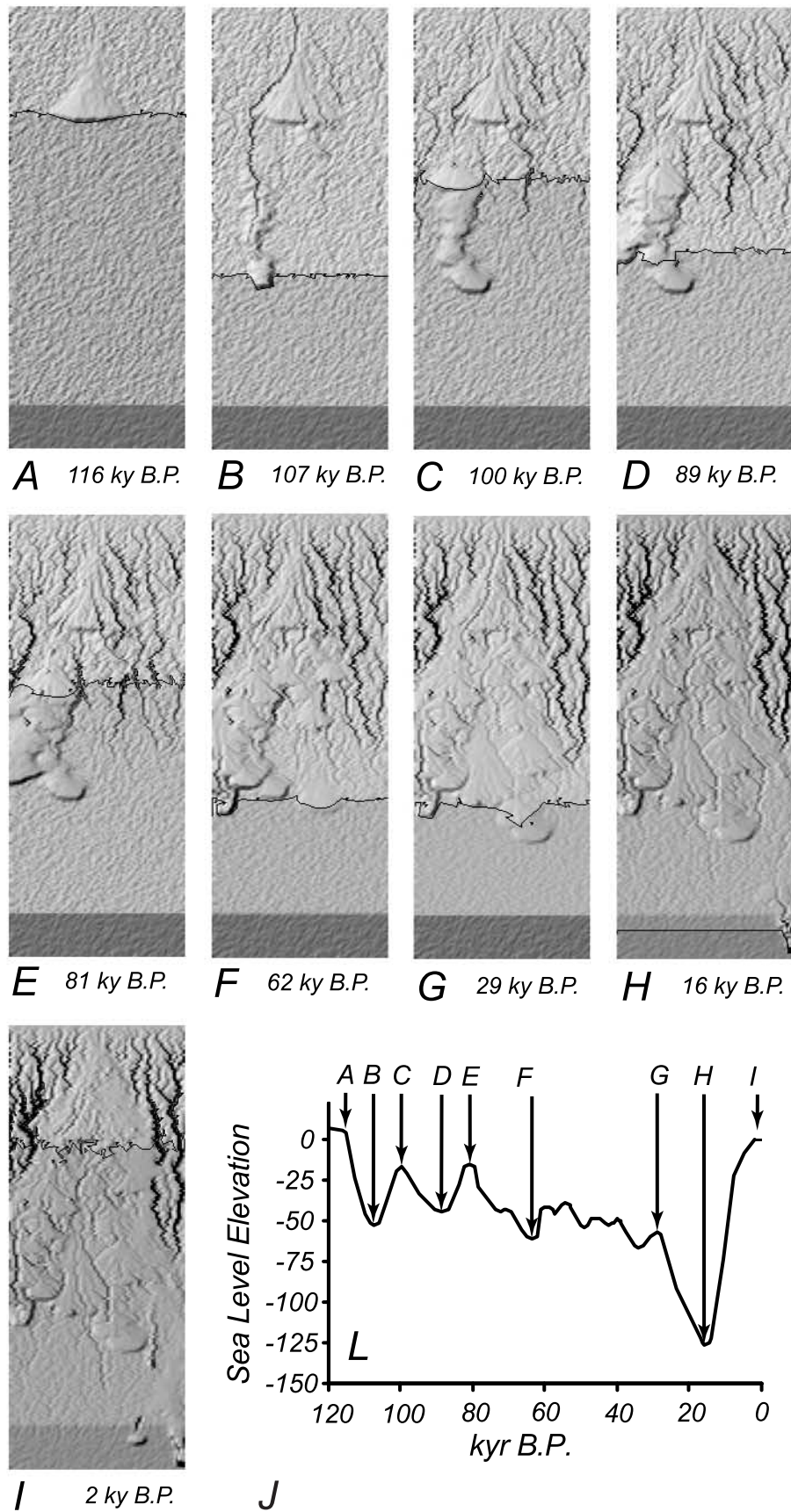


Figure 2

of the last 120 kyr (Figure 2j) shows that sea level changes result in broad, thin deltas with multiple lobes (Figure 2i). In each delta system the river shifts its path during deposition, thus making it difficult to foresee the river location during sea level fall. For example, in Figure 2b the river is located at the right of the delta, but it could move to the left after a relatively short period. The morphology of simulated deltaic deposits is similar to the morphology of observed lobes in the Hudson shelf [Uchupi *et al.*, 2001, Figure 2]. Because of the low gradients on deltaic topsets, fluvial incision on exposed deltas following sea level drop is inhibited relative to nearby continental shelf slopes. Avulsions are uncommon during regressions since deltas extend oceanward while entrenching earlier deposits but occur frequently during sea level rise (Figure 2).

#### 4.2. Response of Fluvial Shelf System to High-Frequency Sea Level Oscillations

[42] In the first simulations we used the long-term record of sea level history deduced from the Papua New Guinea Huon Peninsula sea level data [Chappell *et al.*, 1996]. The Chappell sea level (SL) history has been reconstructed from dated coral reef terraces with few tie points at millennial-scale resolution or higher. Recent studies seem to indicate that the oceanic record of ice volume (hence SL) is much more detailed, with high-frequency fluctuations associated with rapid changes in climate. Oxygen isotope records from Red Sea sediment cores provide a measurement of SL oscillations at a centennial-scale resolution [Siddall *et al.*, 2003]. These data show that sea level has changed during the last glacial cycle at rates up to  $2 \text{ cm yr}^{-1}$ , in correspondence to abrupt changes in climate.

[43] To examine the response of the fluvial-shelf system to high-frequency oscillations of sea level, we ran two simulations with identical initial conditions but with different sea level curves. We first use the low-resolution sea level curve of Fairbanks [1989] for the last 10 kyr. This simulation is then contrasted with a simulation using the sea level curve of Siddall *et al.* [2003]. The Fairbanks [1989] sea level curve was derived from coral reef radiocarbon data with a temporal resolution of thousands of years.

[44] The shelf topography for both simulations is created from 100 points randomly chosen from an initial topography similar to the one used in Figure 1, with size  $200 \times 160 \text{ km}$ . At the top end of the simulation a river with the same characteristics as in the first simulation flows into the domain. The elevations of the selected points are then modified by adding a random elevation uniformly distributed from +10 to -10 m and, finally, interpolated with a kernel smoothing technique to form a regular grid. With this methodology we are able to create an artificial topography that has a system of flat plateaus and depressions with prescribed elevation differences (up to 20 m) that well mimic the topography of the mid-Atlantic shelf. We use this topography to study both incision and aggregation patterns of the establishing fluvial network.

[45] Both simulations start with a sea level at -60 m with respect to the present level, and in both simulations a network of channels form on the shelf, depositing large amounts of sediment in the depressions. In the simulation

with the Fairbanks [1989] SL curve the smooth increase in sea level yields connected sediment deposits that fill the channel incisions in the shelf. As a result, at the end of the simulation (Figure 3b), elongated and uniform sediment prisms are formed on the shelf (compare Figure 3b with Figure 3a). On the contrary, the high-frequency oscillations of the Siddall *et al.* [2003] SL curve lead to sediment deposits that are concentrated in few shelf locations (Figure 3c). In fact, the abrupt changes in sea level do not favor the development of broad and flat deltas; rather, the river deposits are thick and localized due to the rapid change of the river mouth location. As a result, the shelf topography is relatively rough at the end of the simulation (Figure 3c). To better analyze the differences between the two simulations, we subtract the topography of Figure 3c from the topography of Figure 3b (Figure 3e). From this analysis we deduce that several channels produced when sea level was low are not subsequently filled by sediments during sea level rise (narrow light lines in Figure 3e) because the rapid variations in river mouth location cause some depressions to be unfilled. This result has implications for shelf stratigraphy. If sea level varies by several meters at the centennial timescale, a large number of eroded valleys on the shelf will be filled with marine sediment rather than with fluvial or estuarine sediment.

[46] Total channel incision is also dependent on the timescale of sea level oscillations. Abrupt reductions in sea level favor river downcutting, thus increasing the total river incision at the end of the simulation. From Figure 3e we can see that some rivers increase the total incision up to 4 m due to high-frequency sea level oscillations. The deeper incision on the emergent part of the drainage network for the simulation with high-frequency oscillations must occur during the brief time periods when sea level drops below the low-frequency sea level curve.

[47] To study the influence of high-frequency sea level oscillations on channel incision on the shelf, we perform several simulations with a sea level curve that increases linearly from -60 m to 0 m in 10 kyr. We then add a uniformly distributed random oscillation with a period 100 years. By varying the amplitude of the random oscillation, we can quantify the response of the fluvial-shelf system to sea level changes. In Figure 4a we plot the longitudinal profile of the test river indicated in Figure 3 (River X) for different values of the maximum amplitude. A SL rise without oscillations produces a classical concave up profile (Figure 4a). Small-amplitude oscillations still lead to a concave river profile but with a higher incision at the mouth due to river downcutting during the minima of the oscillations. This is because the river filters the small-amplitude oscillations by lowering its bottom uniformly near the mouth without knickpoint retreat. In contrast, when the amplitude of the SL oscillations is large, several knickpoints form at the river mouth and propagate upstream during the simulation (Figure 3a, maximum amplitude of 10, 15, and 20 m). The number of knickpoints and their elevation drop are directly linked to the SL oscillations during in the final stages of the simulation. However, despite the discrete drops in elevation produced by the knickpoints, the total incision at the river mouth is directly proportional to the maximum amplitude of the SL oscillations (Figure 4b).



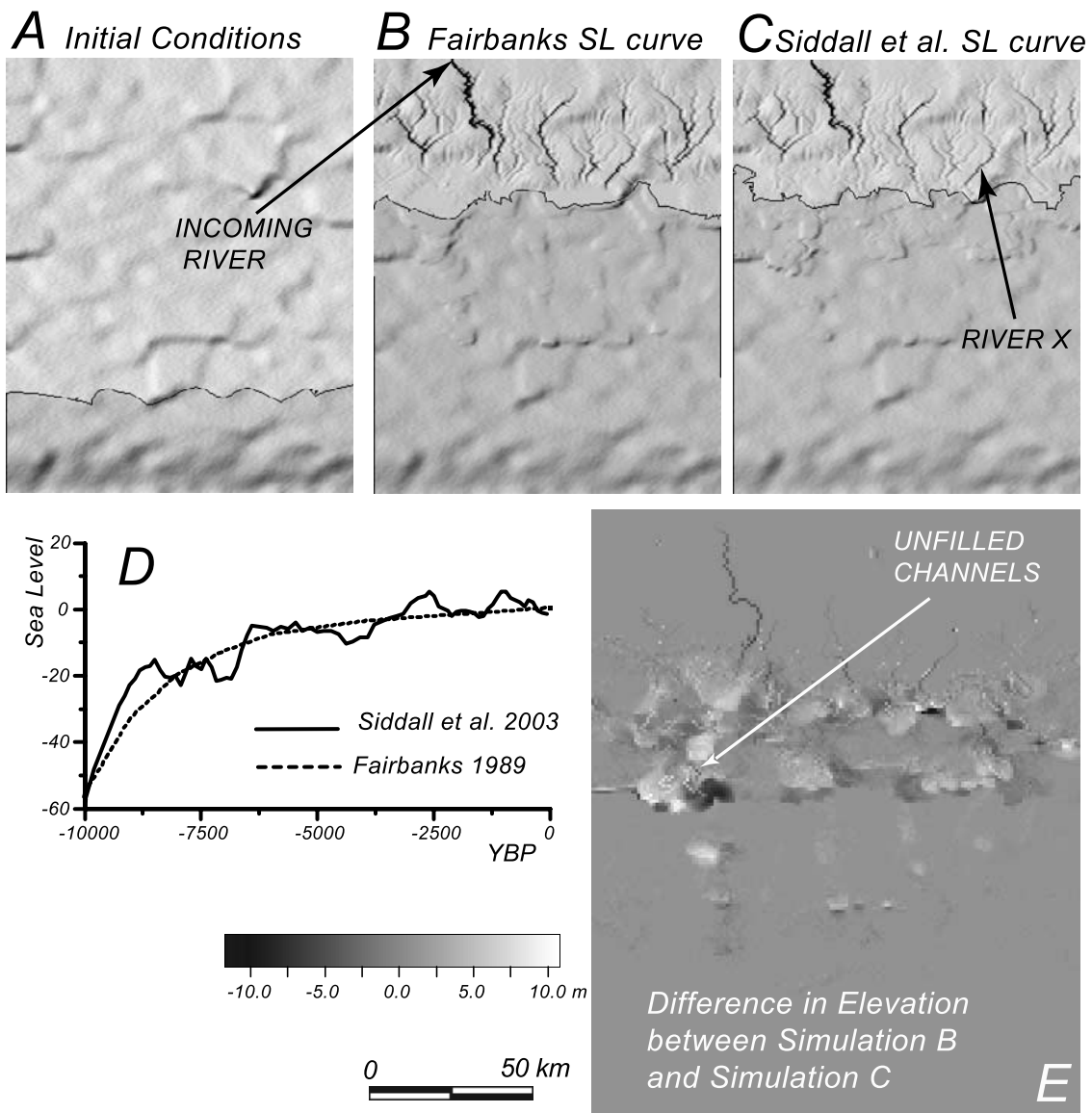


**Figure 3.** Effect of high-frequency oscillations in sea level on fluvial incision of the shelf. (a) Initial shelf topography. (b) Shelf topography after 10,000 years using the *Fairbanks* [1989] SL curve. (c) Shelf topography after 10,000 years using the *Siddall et al.* [2003] SL curve. (d) Comparison between the two SL curves. (e) Elevation difference between the simulation in Figure 3b and the simulation in Figure 3c. High-frequency SL oscillations increase channel incision up to 5 m (dark channels in Figure 3e) and leave several unfilled channels on the shelf (light channels in Figure 3e).

[48] By comparing Figure 1 and Figure 3, we can also qualitatively assess the role of the initial topography on the channel network established on the shelf. On a flat shelf with added random white noise, parallel, elongated valleys form on the shelf (Figure 1). On the other hand, a spatially correlated, random topography like the one used in Figure 3, with large-scale topographic features, favors the aggregation of the newly formed channels into networks reminiscent of the streams dissecting modern coastal plains. Despite the higher aggregation in the second simulation, the newly formed channels still tend to run parallel, following the shelf gradient. We believe that this is caused by the low relief of the shelf topography, which is a result of reworking of the sedi-

ments by waves and currents. Parallel fluvial valleys should be then a common feature of exposed shelves, at least in the first phase of the network development.

#### 4.3. Effect of Varying Sediment Load and Runoff

[49] Variations in sediment load and runoff also affect deposition and channel development. To estimate possible variations in sediment load, we utilize the global cyclostratigraphy approach developed by *Perlmutter and Matthews* [1989; *Perlmutter et al.*, 1998]. In this framework the sediment load of a river is intrinsically associated with climatic successions, whereas climatic successions strongly depend on the geographic position of the river basin and are not necessarily synchronous with glacioeustatic sea level

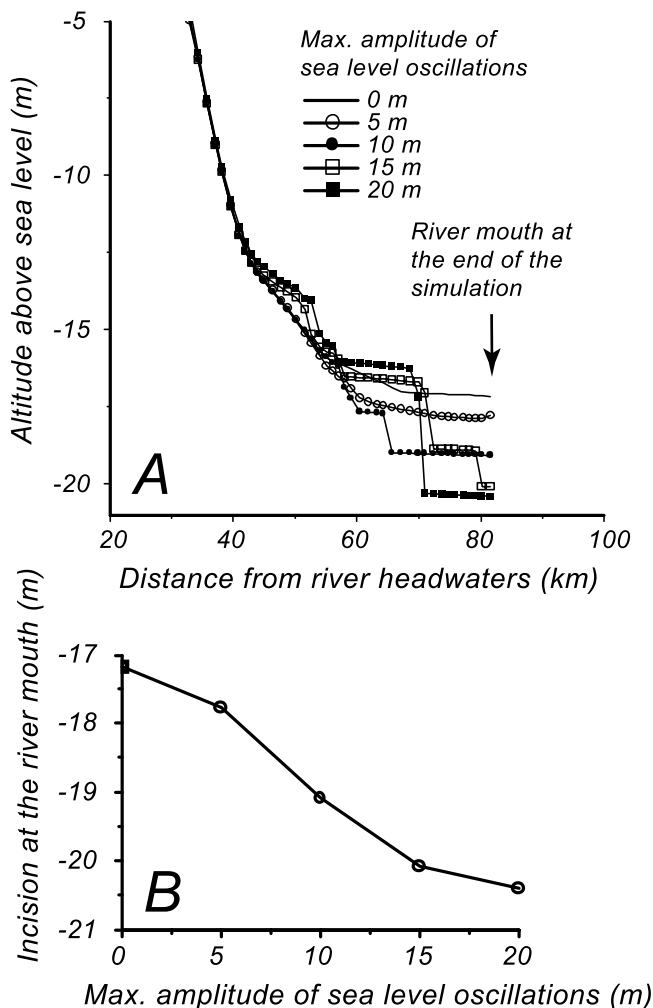


**Figure 4.** (a) Longitudinal profiles of the river indicated in Figure 3a. Each longitudinal profile is calculated after a simulation with a linear sea level curve with superimposed random SL oscillations of determined amplitude (from 0 to 20 m). (b) Total incision at the river mouth as a function of the amplitude of SL oscillations.

cycles. For example, tropical-humid areas can become temperate-arid during a climatic minimum (glaciation), with a decrease in sediment yield, whereas temperate-dry areas can become polar-humid, with an increase in sediment yield. In Figure 5 we compare a simulation with a river having a constant total sediment load of  $400,000 \text{ m}^3 \text{ yr}^{-1}$  and a constant mean annual discharge of  $450 \text{ m}^3 \text{ s}^{-1}$  (Figures 5a and 5b) to a simulation with a river with varying discharge and sediment load (Figures 5c and 5d). The size of the domain is  $200 \times 80 \text{ km}$ , with an added random noise elevation. In both simulations the ocean level oscillates along the curve shown in Figure 5e. In Figures 5c and 5d the sediment load and discharge are modified according to the estimates provided by *Perlmutter et al.* [1998] for tropical-dry regions (Figures 5f and 5g). In this climatic belt a climatic minimum produces a temperate subhumid climate, with an increase in sediment load (Figure 5f).

[50] A constant sediment load does not favor avulsion along the river course but localizes it to the delta area,

where sediments are deposited. During SL rise the rivers do not change their pattern, and the fluvial incisions are completely filled by deltaic deposits (Figures 5a and 5b). From the simulations it is clear that an increase in sediment load in the river favors avulsion (Figures 5c and 5d). In fact, during SL low stands the higher sediment load produces aggradation along the river until the river bottom reaches the elevation of the surrounding coastal plain. At this point the river finds a new course, discharging the sediments in a different location along the coastline (Figures 5c and 5d). The increased sediment load yields broad deposits on the shelf, with higher burial potential near the coastline (Figure 5d). Thus an increase in sediment load has a twofold effect on channel incision and channel burial on the shelf: it increases the number of incised rivers by avulsion and favors the burial of the channels near the coastline. The coupling of these model results with the cyclostratigraphic framework of *Perlmutter and Matthews* [1989] determines, for each climatic belt, the periods (corresponding to sediment load maxima) of the formation of new incisions and the locations on the shelf (corresponding to the coastline location when the maxima in sediment load occur) where the incisions are filled with estuarine and fluvial deposits.

#### 4.4. Effect of Shelf Morphology

[51] Morphological features such as submarine canyons that dissect the shelf slope break and large sand ridges that are present on the shelf will affect channel incision and network development. Submarine canyons, which convey sediments by gravity-driven processes [*McAdoo et al.*, 2000], might represent a favorable location for subaerial channel incision. Although it is realistic to suppose that channels will form by headward retreat once the canyon scarps are exposed to rainfall action, this does not automatically imply that the major rivers crossing the shelf will discharge into them. In reality, simulations indicate that the rivers are almost unaffected by the canyon presence (Figure 6, domain size  $270 \times 120 \text{ km}$ , with random noise) because the aggregation of the riverine network is mostly dictated by the local and upstream watershed distribution, and during sea level fall, canyons that are still below sea level have negligible influence on subaerial channel incision and deltaic deposition. In other words, if the shelf topography is reworked during sea level rise, the major rivers will very likely excavate a new path on the shelf during sea level retreat and at the latest stages of marine regression, only if they are very close to a canyon, will change their course toward it. However, if previously excavated channels or canyons extend across the entire continental shelf, as is the case with the submerged Hudson River valley, they will have a greater impact on the riverine planforms because of direct interaction with channel formation.

[52] Contrary to expectation, the head of the submarine canyon does not significantly enlarge after exposure. Careful analysis of available bathymetric data (NGDC Coastal Relief Model) reveals that the average slope of the upper part (above  $-120 \text{ m}$  with respect to mean sea level) of the canyons in the Virginia shelf is around 0.05. This value is considerably higher than the average slope of the shelf (0.008) but can be considered gentle for

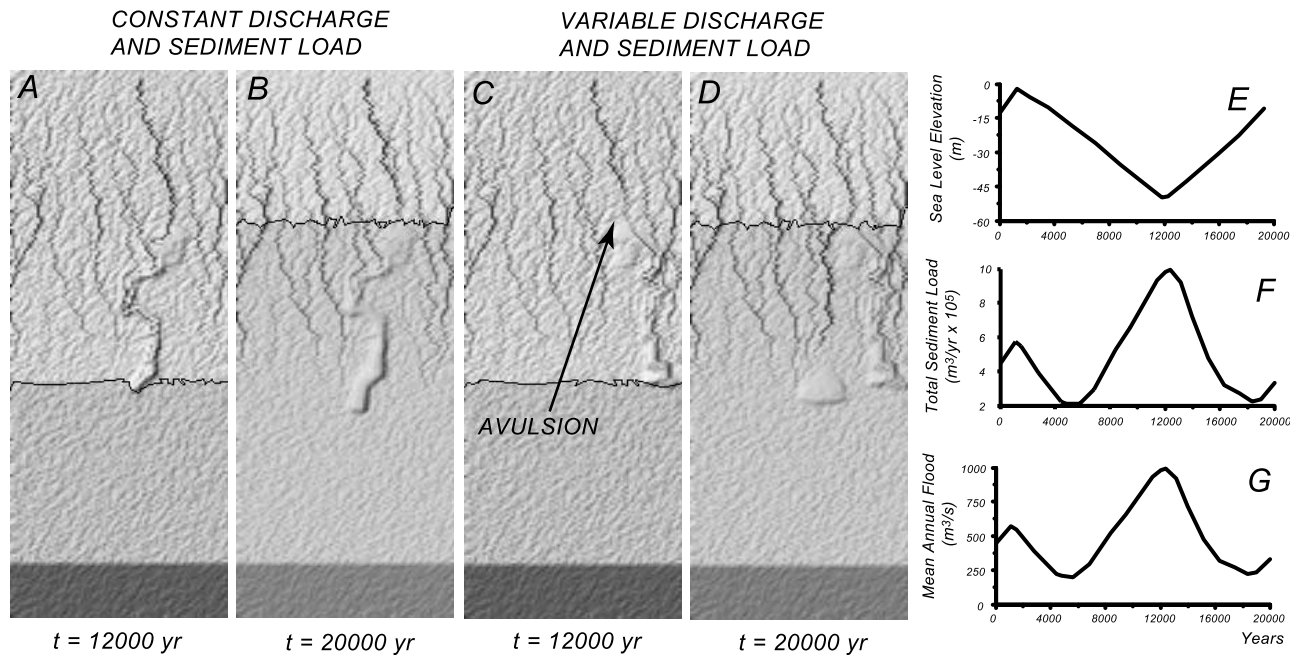


**Figure 5.** Comparison between a simulation with constant river runoff and sediment load and a simulation with variable river runoff and sediment load. Simulation parameters and shelf geometry are identical to the simulation of Figure 2. River runoff and sediment load are assumed to increase following the estimates of *Perlmutter and Matthews* [1989] for tropical-dry regions. (a, b) Results with constant river discharge and sediment load at  $t = 12,000$  years and  $t = 20,000$  years, respectively. (c, d) Results with variable river discharge and sediment load. (e) Sea level elevation as a function of time for both simulations. (f) Mean annual flood as a function of time for the second simulation. The mean annual flood is assumed constant and equal to  $450 \text{ m}^3 \text{ s}^{-1}$  for the first simulation. (g) Total sediment load as a function of time for the second simulation. The total sediment load is assumed constant and equal to  $400,000 \text{ m}^3 \text{ yr}^{-1}$  for the first simulation.

subaerial processes (hillslopes normally reach a value of 0.3). Mass wasting processes are thus inhibited or do not mobilize large amounts of material. Mass wasting processes might have a critical role when sea level is lower, exposing the steep part of the continental edge. The only way to enlarge the canyon head in a short period of time is by headwater erosion of fluvial streams, but this is only possible if channels with enough discharge are flowing into the canyon. As just discussed, it is the aggregation of the upstream drainage area that influences the path of the river during falling sea level and not the topography of the continental edge. Therefore only in specific situations can we expect that a large river extending across the shelf during sea level regression would flow into a preexisting canyon.

[53] To explore the influence of topography on sediment redistribution and channel incision, we perform a simulation utilizing the present shelf bathymetry offshore of the Virginia portion of the Delmarva Peninsula (domain size  $110 \times 110$  km, mesh size 500 m, Figure 7). Large-scale bed forms (sand ridges) run from northeast to southwest on the continental shelf. It is questionable whether this topography would be preserved during sea level fall because high-energy near-shore processes would most likely rework sediment near the coastline. This notwithstanding, the objective of the simulation is to explore the influence of preexisting topography, which has subtle but large-scale

relief, upon patterns of incision and deposition during sea level fall.

[54] In these simulations we assume a constant rate of sea level change equal to the average rate of SL fall during the Wisconsin glaciation (Figure 7). After 20,000 years, simulation results show that a reticulate network of channels is established on the shelf surface (Figure 7d). Initial topography strongly influences drainage patterns. In particular, the presence and orientation of sand ridges constrain the channels to run parallel to these large-scale bed forms. In the transition from a submerged topography to a subaerial topography, most depressions are filled and eventually integrated into the drainage system. Near river outlets, depressions are first filled (partly or totally) by the sediment deposited in the delta. Once these areas become emergent, the channel network will close the last depressions, building an integrated network.

[55] The main drainage pattern is established very early in the simulation, testifying to the role of initial conditions in the network development. The drainage network is initially strongly fragmented but gradually becomes integrated. At the first stages of the simulation, there are many examples of “gullies” eroding headward from initial scarps. These headwater dissections are initially largely independent of downstream erosion and deposition. Moreover, some relatively low-lying locations change from initial deposition to erosion as incised channels migrate headward into the



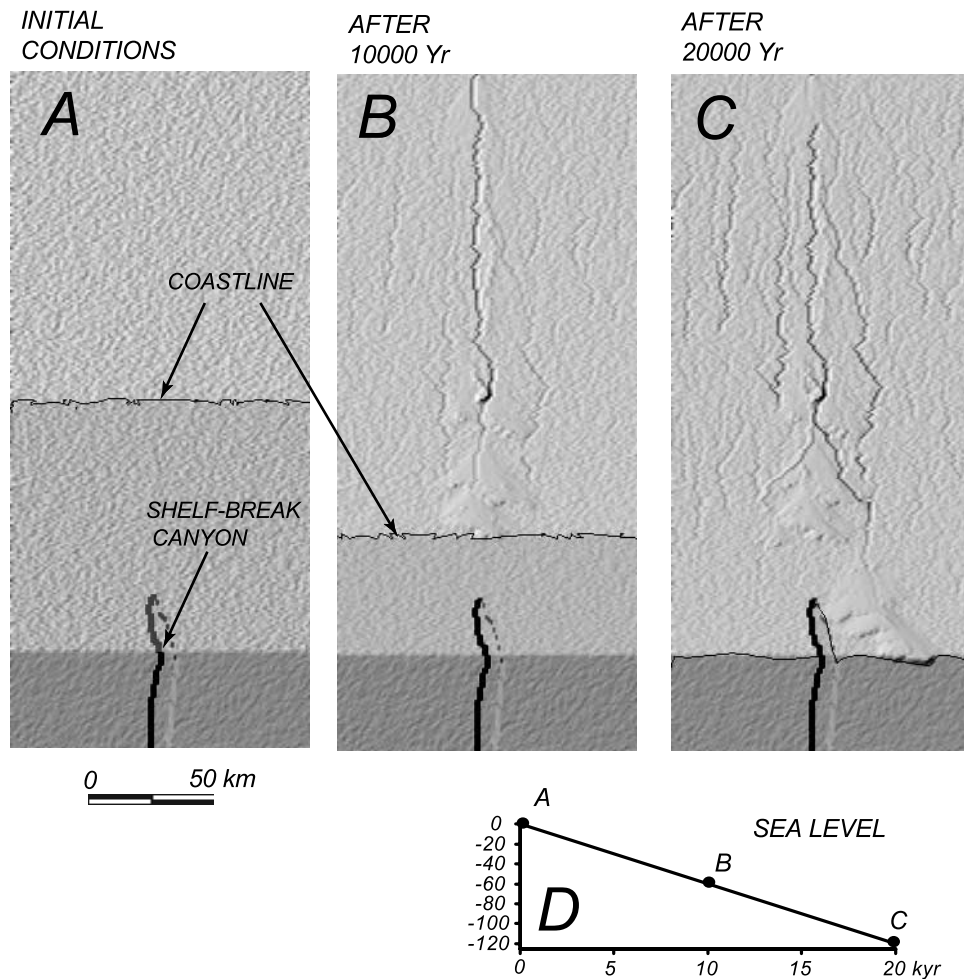


**Figure 6.** Influence of submarine canyons, located in the continental slope, on the establishing channels. The river path, determined by the upstream watershed characteristics, local topography, and sediment deposits seems to be unaffected by the presence of the canyon. (a) Initial conditions. (b) After 10,000 years. The coastline is close to the submarine canyon. (c) After 20,000 years. The river is not captured by the canyon, mostly because its course is regulated by the shape of the deltaic deposits. (d) Sea level curve. In the simulation, sea level fall occurs at a constant rate equal to the averaged value during the Wisconsin glaciation (see Figure 3).

location. At the end of the simulation we note that most dissection occurs in few major channels.

## 5. Discussion and Conclusions

[56] Sea level oscillations, climatic variations, and shelf topography influence the development of fluvial features on the continental shelf during sea level variations. We have used a numerical model, parameterized with Virginia coastal plain data, in order to understand the specific role of each of these processes and quantify their influence on channel formation and incision. Model results show that the detailed structure of sea level oscillations is important for sediment redistribution and channel changes. In particular, high-frequency SL oscillations, which seem to have occurred in the last glacial cycle, increase fluvial incision in the terminal reaches of the rivers due to rapid downcutting during the low stands of the oscillation. Through a series of numerical simulations, we show that

oscillations of small amplitude are filtered by the fluvial system, producing a spatially uniform lowering of the river bottom. On the other hand, oscillations of high amplitude (up to 20 m) form a series of small knickpoints (up to 3 m) that propagate upstream and dissipate rapidly. However, the total incision at the river mouth is directly proportional to the oscillation amplitude both with and without knickpoints.

[57] Furthermore, simulations show that an increase in river sediment load driven by climatic change favors channel avulsion with the formation of new fluvial incisions on the shelf. At the same time a higher sediment load leads to a higher potential for burial by fluvial deposition.

[58] The initial shelf topography strongly influences the future development of the channel network. During the simulations the drainage network is initially strongly fragmented but gradually becomes integrated through depression infilling and dissection of steep scarps. Coastal

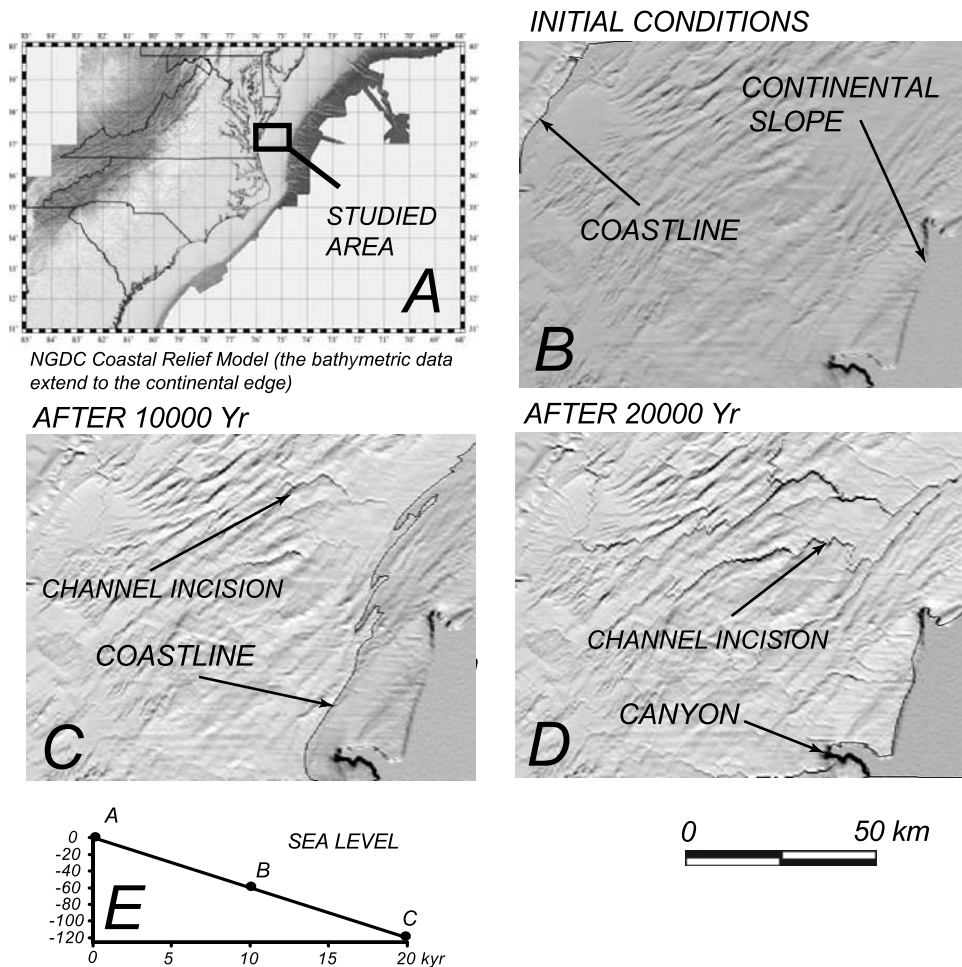


**Figure 7.** Simulation of channel formation in the continental shelf using the current shelf topography. (a) Location of the study area offshore of the Virginia portion of the Delmarva Peninsula. (b) Initial conditions with the entire shelf submerged. (c) Formation of a channel network and infilling of depressions after 10,000 years. (d) Channel incision increases when the coastline is below the shelf slope (after 20,000 years). (e) Sea level curve (constant sea level fall).

processes, not incorporated in the present formulation, will be of crucial importance for sediment redistribution and shelf topography modification during sea level oscillations. These processes are now being incorporated into this model.

[59] Results show that there are three types of channel development on the exposed shelf. The first type are “local” channels that originate on the shelf and are slightly incised, producing small erosional dendritic networks. The pattern of these channels is strongly affected by the local topography of the shelf since the reduced deposition does not favor channel avulsion. We can define the corresponding fluvial incision as “local fluvial incision.” The second type are large channels originating from onshore areas that create deltas and larger incisions. Their thick, broad deposits consistently modify the shelf morphology, leading to frequent avulsions during marine transgressions. The strong feedbacks between deltaic deposition, avulsion, channel location, and sea level oscillations are so complex that it is difficult to foresee the development of the channels during sea level fall. Simulations with slightly different initial conditions pro-

duce different outcomes in terms of channel location. As a consequence, shelf incision by large channels becomes chaotic and highly variable in space and time. We define this incision as “fluvial incision driven by deltaic deposits.” The third type is the formation of channels at the shelf edge when sea level drops below it, with channel incision caused by headward migration of knickpoints. Because the sediment load of these channels is discharged into the continental slope, avulsion is impossible, and the channels maintain a fixed position during their development. The temporal evolution of the channels, rather than their spatial evolution, is morphologically important since the degree of incision and the knickpoint location will depend on the duration of sea level low stands. We define the corresponding incision as “locked fluvial incision” since the position of the channels does not vary in time.

## Appendix A

[60] In this appendix we describe in detail the parameterization of fluvial processes in the landscape evolution

model. Two fundamental assumptions are made. The first is that discharge is proportional to upstream drainage area in every mesh element. Water discharge can be related to drainage area through the equation

$$Q = K_a A^e, \quad (\text{A1})$$

where  $e$  is a parameter less than unity that keeps in account the increase of rainfall intensity for small areas;  $K_a$  and  $e$  also vary as a function of climatic conditions. The second assumption is that river dimensions vary downstream following the rules of hydraulic geometry [Leopold and Maddock, 1953] in the sense that river width, depth, and velocity are related to bankfull discharge:

$$D = K_D Q^a, \quad (\text{A2a})$$

$$W = K_w Q^b, \quad (\text{A2b})$$

$$V = K_V Q^c, \quad (\text{A2c})$$

where  $D$  and  $W$  are river depth and width, respectively, and  $V$  is water velocity. From studies carried out in the Pennsylvania coastal plains, Brush [1961] derived a set of values for the parameters in equations (A1) and (A2) (see Table 1).

[61] Two mechanisms produce channel incision or aggradation. In reaches where the amount of alluvium from upstream is less than the transport capacity of the river the current extracts sediment from the underlying bedrock. Following Howard and Kerby [1983], the rate of incision can be posed proportional to bottom shear stress by

$$\frac{\partial z}{\partial t} = -K_T(\tau - \tau_c), \quad (\text{A3})$$

where  $z$  is the bottom elevation,  $\tau$  is the shear stress at the bottom of the bedrock channel, and  $\tau_c$  the critical shear stress for erosion. In order to define  $\tau$  in terms of drainage area and channel gradient, we proceed as follows. Considering a uniform flow and a rectangular channel cross section, the following relationships hold:

$$\tau = \gamma D S, \quad (\text{A4})$$

$$V = D^{2/3} S^{1/2} / N, \quad (\text{A5})$$

$$Q = D W V, \quad (\text{A6})$$

where  $S$  is the channel gradient and  $N$  is the Manning coefficient. Utilizing equations (A1), (A2b), (A4), (A5), and (A6), equation (A3) becomes

$$\frac{\partial z}{\partial t} = -K_T \left( K_a A^{0.6e(1-b)} S^{0.7} - \tau_c \right), \quad (\text{A7})$$

where

$$K_Z = \gamma \left( \frac{N K_a^{1-b}}{K_w} \right)^{3/5}. \quad (\text{A8})$$

If we use a Manning coefficient  $N$  of  $0.03 \text{ s m}^{-1/3}$  and a water weight of  $9800 \text{ N m}^{-3}$ , we obtain a value  $K_Z = 932.0 \text{ kg m}^{-1.422} \text{ s}^2$ . From erosion studies in Virginia badlands we can furthermore specify the parameter  $K_T$  that is responsible for the rate of bedrock channel incision. Substituting in equation (A7) the discharge and incision rate reported by Howard and Kerby [1983], a value of  $K_T = 0.015 \text{ m}^3 (\text{N yr})^{-1}$  is obtained.

[62] For alluvial channels the rate of erosion or deposition in each river reach equals the divergence of the volumetric sediment discharge. If an area  $\alpha$  is considered (i.e., a grid cell), then the variations in bottom elevation depend on the incoming volume of sediment per unit time  $Q_{sb}^{\text{in}}$  and the outgoing volume  $Q_{sb}^{\text{out}}$ :

$$\frac{\partial z}{\partial t} = \frac{1}{\alpha} (Q_{sb}^{\text{in}} - Q_{sb}^{\text{out}}). \quad (\text{A9})$$

The volumetric sediment discharge  $Q_{sb}$  can be expressed with a steady state total load or bed load equation. In the Einstein-Brown formula [Rouse, 1950] the volumetric sediment discharge is linked to the bottom shear stress with the relationship

$$\phi = (1/\psi)^3, \quad (\text{A10})$$

where the nondimensional parameters  $\phi$  and  $\psi$  are

$$\phi = \frac{Q_{sb}}{W \omega d (1 - \mu)} \quad \frac{1}{\psi} = \frac{\tau}{(\gamma_s - \gamma) d}, \quad (\text{A11})$$

with  $\mu$  being the bed porosity,  $\omega$  the sediment fall velocity,  $d$  the sediment grain size, and  $\gamma_s$  the unit weight of sediment grains. Utilizing equations (A11), (A2b), (A4), (A5), and (A6), we obtain the expression

$$Q_{sb} = K_q A^{eb} \left( K_v A^{0.6e(1-b)} S^{0.7} \right)^3, \quad (\text{A12})$$

with

$$K_q = \frac{K_e \omega (1 - \mu) K_w K_a^b}{(\gamma_s - \gamma)^3 d^2} \quad K_v = \gamma \left( \frac{N K_a^{1-b}}{K_w} \right)^{0.6}. \quad (\text{A13})$$

Considering sand with diameter  $d = 0.2 \text{ mm}$ , fall velocity  $\omega = 2.3 \times 10^{-3} \text{ m s}^{-1}$ , sediment weight per unit volume  $\gamma_s = 2650 \text{ kg m}^{-3}$ , and bed porosity  $m = 0.5$ , we obtain the values  $K_v = 15.0 \text{ m}^{2.104} \text{ yr}^{-1}$  and  $K_q = 288.0 \text{ m}^{-0.422}$ . It is important to note that the sediment load expressed through equation (A12) is relative to a constant water discharge, whereas river flow is intrinsically variable in time. In our model the parameter  $K_q$  has been calculated considering that the dominant discharge has the same order of magnitude of the annual flood [Wolman and Miller, 1960]. Furthermore, we assume that bed load sediment transport is equal to 10% of the total load. The volume of sediment carried by bed load



and suspended sediment transport is used to build the delta lobes in the shelf, whereas wash load is dispersed in the water column and is not accounted for in these simulations. However, part of the fine-grained fluvial sediments will be deposited on the shelf, thus contributing to erase the preexisting channel topography. This component will be added to the model in the future.

[63] For efficiency in computation the simulation model assumes that alluvial stream gradients equal the equilibrium value for a stream graded to a constant elevation base level for the specified inputs of sediment load and discharge. In other words, transient nonequilibrium gradients in response to changes in base level or sediment and water input are not simulated. The error associated with this assumption during sea level changes can be assessed in two ways. Howard [1982] simulated the transient response of sand bed alluvial stream channels to changes in hydraulic regime and base level. The time,  $T$ , required for 95% readjustment of gradient to a step change in base level to a spatially fixed downstream control point was found to be

$$T = 1.8 \frac{L^2 S}{2q_s}, \quad (\text{A14})$$

where  $q_s$  is the bed sediment discharge per unit channel width ( $\sim 4800 \text{ m}^2 \text{ yr}^{-1}$  for a Delaware-sized river),  $L$  is the channel length subject to regrading (assumed to be 100 km), and  $S$  is the channel gradient (assumed equal to the shelf gradient of  $\sim 0.0008$ ). The resulting timescale is  $\sim 1500$  years. Another check is to calculate the change in channel gradient required for a stream eroding at steady state in response to a constant rate of base-level change with respect to a stream at steady state with a fixed base level. From equation (5), equilibrium channel gradient,  $S$ , is approximately proportional to the square root of sediment discharge,  $Q_s$ , for sand bed streams. If an alluvial stream of length  $L$  downcuts at a constant rate  $\partial z/\partial t$ , then the additional sediment load is  $-\partial z/\partial t LW$ , where  $W$  is the channel width and the fractional change in channel gradient  $\Delta S$  is

$$\Delta S \cong \frac{(Q_s - \partial z/\partial t LW)^{0.5} - Q_s^{0.5}}{Q_s^{0.5}}. \quad (\text{A15})$$

Here we assume, as along the mid-Atlantic coast, that upstream incision is limited in headward extent by a bedrock fall line. For a Delaware-sized river of width  $\sim 170$  m the fractional gradient change for the time period from  $\sim 120,000$  B.P. to  $\sim 90,000$ , when sea level dropped  $\sim 60$  m (although not steadily), the fractional gradient change is  $\sim 0.7\%$ . For the rapid drop of  $\sim 60$  m over 15,000 years after 30,000 B.P. the fractional gradient change is  $\sim 6\%$ . Both analyses suggest that the steady state assumption does not lead to large errors. In actuality, nonsteady state gradient biases are even smaller than the above analysis, which is based upon the assumption of a spatially fixed base level control. Because of the low gradient of continental shelves, channels shorten for base level rises and lengthen during falling sea level, reducing the effects of base level change on gradients.

[64] **Acknowledgments.** Support for this study was provided by the Office of Naval Research, Geocutter Program, grant N00014-00-1-0822

and by the Office of Naval Research, EuroStrataform Program, grant N00014-03-C-0134. We also thank Robert Anderson, Mike Ellis, Chris Paola, Torbjörn Törnqvist, and Joseph Donoghue for constructive comments; their suggestions significantly improved the paper.

## References

- Best, J. L., and P. J. Ashworth (1997), Scour in large braided rivers, and the recognition of sequence stratigraphic boundaries, *Nature*, **387**(6630), 275–277.
- Blum, M. D., and T. E. Törnqvist (2000), Fluvial responses to climate and sea-level change: A review and look forward, *Sedimentology*, **47**, suppl. 1, 2–48.
- Brush, L. M., Jr. (1961), Drainage basins, channels, and flow characteristics of selected streams in central Pennsylvania, *U.S. Geol. Surv. Prof. Pap.*, **282-F**.
- Butcher, S. W. (1990), The nickpoint concept and its implications regarding onlap to the stratigraphic record, in *Quantitative Dynamic Stratigraphy*, edited by T. A. Cross, pp. 375–385, Pearson, New York.
- Carson, M. A., and M. J. Kirkby (1972), *Hillslope Form and Process*, 475 pp., Cambridge Univ. Press, New York.
- Chappell, J., A. Omura, T. Esat, M. McCulloch, J. Pandolfi, Y. Ota, and B. Pillans (1996), Reconciliation of late Quaternary sea levels derived from coral terraces at Huon Peninsula with deep sea oxygen isotope records, *Earth Planet. Sci. Lett.*, **141**(1–4), 227–236.
- Chen, Z. Q., C. H. Hobbs, J. F. Wehmiller, and S. M. Kimball (1995), Late Quaternary paleochannel systems on the continental-shelf, south of the Chesapeake bay entrance, *J. Coastal Res.*, **11**(3), 605–614.
- Dalrymple, R. W., R. Boyd, and B. A. Zaitlin (1994), Preface, *Spec. Publ. SEPM Soc. Sediment. Geol.*, **51**, iii.
- Davies, T. A., and J. A. Austin (1997), High resolution 3D seismic reflection and coring techniques applied to late Quaternary deposits on the New Jersey shelf, *Mar. Geol.*, **143**(1–4), 137–149.
- Duncan, C. S., J. A. Goff, J. A. Austin, and C. S. Fulthorpe (2000), Tracking the last sea-level cycle: Seafloor morphology and shallow stratigraphy of the latest Quaternary New Jersey middle continental shelf, *Mar. Geol.*, **170**(3–4), 395–421.
- Fagherazzi, S., A. D. Howard, and P. L. Wiberg (2002), An implicit finite difference method for drainage basin evolution, *Water Resour. Res.*, **38**(7), 1116, doi:10.1029/2001WR000721.
- Fairbanks, R. G. (1989), A 17,000-year glacio-eustatic sea-level record—Influence of glacial melting rates on the younger dryas event and deep-ocean circulation, *Nature*, **342**(6250), 637–642.
- Fisk, H. N. (1944), *Geological Investigation of the Alluvial Valley of the Lower Mississippi River*, Miss. River Comm., Vicksburg, Miss.
- Foyle, A. M., and G. F. Oertel (1997), Transgressive systems tract development and incised-valley fills within a Quaternary estuary-shelf system: Virginia inner shelf, USA, *Mar. Geol.*, **137**(3–4), 227–249.
- Hallet, B., L. Hunter, and J. Bogen (1996), Rates of erosion and sediment evacuation by glaciers: A review of field data and their implications, *Global Planet. Change*, **12**(1–4), 213–235.
- Howard, A. D. (1982), Equilibrium and time scales in geomorphology—Application to sand-bed alluvial streams, *Earth Surf. Processes Landforms*, **7**(4), 303–325.
- Howard, A. D. (1994), A detachment-limited model of drainage-basin evolution, *Water Resour. Res.*, **30**(7), 2261–2285.
- Howard, A. D. (1997), Badland morphology and evolution: Interpretation using a simulation model, *Earth Surf. Processes Landforms*, **22**(3), 211–227.
- Howard, A. D., and G. Kerby (1983), Channel changes in badlands, *Geol. Soc. Am. Bull.*, **94**, 739–752.
- Jenson, S. K., and J. O. Domingue (1988), Extracting topographic structure from digital elevation data for geographic information systems analysis, *Photogramm. Eng. Remote Sens.*, **54**(11), 1593–1600.
- Jervey, M. T. (1988), Quantitative geological modeling of siliciclastic rock sequences and their seismic expression, *Spec. Publ. Soc. Econ. Paleontol. Mineral.*, **42**, 47–69.
- Knebel, H. J., S. A. Wood, and E. C. Spiker (1979), Hudson river—Evidence for extensive migration of the exposed continental-shelf during Pleistocene time, *Geology*, **7**(5), 254–258.
- Knox, J. C. (1983), Responses of river systems to Holocene climates, in *Late Quaternary Environments of the United States*, vol. 2, *The Holocene*, edited by H. E. Wright and S. C. Porter, pp. 26–41, Univ. of Minn. Press, Minneapolis, Minn.
- Knox, J. C. (1993), Large increases in flood magnitude in response to modest changes in climate, *Nature*, **361**(6411), 430–432.
- Langbein, W. B., and S. A. Schumm (1958), Yield of sediment in relation to mean annual sediment, *Eos Trans. AGU*, **39**, 1076–1084.
- Leeder, M. R., T. Harris, and M. J. Kirkby (1998), Sediment supply and climate change: Implications for basin stratigraphy, *Basin Res.*, **10**(1), 7–18.

- Leopold, L. B., and W. B. Bull (1979), Base level, aggradation, and grade, *Proc. Am. Philos. Soc.*, 123, 168–202.
- Leopold, L. B., and T. Maddock (1953), The hydraulic geometry of stream channels and some physiographic implications, *U. S. Geol. Surv. Prof.*, 252.
- Marr, J. G., J. B. Swenson, C. Paola, and V. R. Voller (2000), A two-diffusion model of fluvial stratigraphy in closed depositional basins, *Basin Res.*, 12(3–4), 381–398.
- McAdoo, B. G., L. F. Pratson, and D. L. Orange (2000), Submarine landslide geomorphology, US continental slope, *Mar. Geol.*, 169(1–2), 103–136.
- Meijer, X. D. (2002), Modelling the drainage evolution of a river-shelf system forced by Quaternary glacio-eustasy, *Basin Res.*, 14(3), 361–377.
- Milliman, J. D., and J. P. M. Syvitski (1992), Geomorphic tectonic control of sediment discharge to the ocean—The importance of small mountainous rivers, *J. Geol.*, 100(5), 525–544.
- Mohrig, D., P. L. Heller, C. Paola, and W. J. Lyons (2000), Interpreting avulsion process from ancient alluvial sequences: Guadalope-Mataranya system (northern Spain) and Wasatch Formation (western Colorado), *Geol. Soc. Am. Bull.*, 112(12), 1787–1803.
- Paola, C., P. L. Heller, and C. L. Angevine (1992), The large-scale dynamics of grain-size variation in alluvial basins, 1: Theory, *Basin Res.*, 4, 73–90.
- Perlmutter, M. A., and M. D. Matthews (1989), Global cyclostratigraphy: A model, in *Quantitative Dynamic Stratigraphy*, edited by T. Cross, pp. 233–260, Prentice-Hall, Old Tappan, N. J.
- Perlmutter, M. A., B. J. Radovich, M. D. Matthews, and C. G. St. C. Kendall (1998), The impact of high-frequency sedimentation cycles on stratigraphic interpretation, in *Sequence Stratigraphy—Concepts and Applications*, NPF Spec. Publ. 8, edited by F. M. Gradstein, K. O. Sandvik, and N. J. Milton, pp. 141–170, Elsevier Sci., New York.
- Probst, J. L. (1989), Hydroclimatic fluctuations of some European rivers since 1800, in *Historical Changes of Large Alluvial River, Western Europe*, edited by G. E. Petts, pp. 41–55, John Wiley, Hoboken, N. J.
- Roering, J. J., J. W. Kirchner, and W. E. Dietrich (1999), Evidence for nonlinear, diffusive sediment transport on hillslopes and implications for landscape morphology, *Water Resour. Res.*, 35(3), 853–870.
- Rouse, H. (1950), *Engineering Hydraulics*, John Wiley, Hoboken, N. J.
- Salter, T. (1993), Fluvial scour and incision: Models for their influence on the development of realistic reservoir geometries, *Geol. Soc. Spec. Publ.*, 73, 33–51.
- Schumm, S. A. (1993), River response to baselevel change: Implications for sequence stratigraphy, *J. Geol.*, 101(2), 279–294.
- Shanley, K. W., and P. J. McCabe (1994), Perspectives on the sequence stratigraphy of continental strata, *Am. Assoc. Petrol. Geol. Bull.*, 78, 544–568.
- Siddall, M., E. J. Rohling, A. Almogi-Labin, C. Hemleben, D. Meischner, I. Schmelzer, and D. A. Smeed (2003), Sea-level fluctuations during the last glacial cycle, *Nature*, 423(6942), 853–858.
- Summerfield, M. A. (1985), Plate tectonics and landscape development on the African continent, in *Tectonic Geomorphology*, edited by M. Morisawa and J. Hack, pp. 27–51, Allen and Unwin, Concord, Mass.
- Sun, T., C. Paola, G. Parker, and P. Meakin (2002), Fluvial fan deltas: Linking channel processes with large-scale morphodynamics, *Water Resour. Res.*, 38(8), 1151, doi:10.1029/2001WR000284.
- Syvitski, J. P. M., S. D. Peckham, R. Hilberman, and T. Mulder (2003), Predicting the terrestrial flux of sediment to the global ocean: A planetary perspective, *Sediment. Geol.*, 162(1–2), 5–24.
- Talling, P. J. (1998), How and where do incised valleys form if sea level remains above the shelf edge?, *Geology*, 26(1), 87–90.
- Twichell, D. C., H. J. Knebel, and D. W. Folger (1977), Delaware River—Evidence for its former extension to Wilmington submarine canyon, *Science*, 195(4277), 483–485.
- Uchupi, E., N. Driscoll, R. D. Ballard, and S. T. Bolmer (2001), Drainage of late Wisconsin glacial lakes and the morphology and late quaternary stratigraphy of the New Jersey–southern New England continental shelf and slope, *Mar. Geol.*, 172(1–2), 117–145.
- van Heijst, M. W. I. M., and G. Postma (2001), Fluvial response to sea-level changes: A quantitative analogue, experimental approach, *Basin Res.*, 13(3), 269–292.
- van Heijst, M. W. I. M., G. Postma, X. D. Meijer, J. N. Snow, and J. B. Anderson (2001), Quantitative analogue flume-model study of river-shelf systems: Principles and verification exemplified by the Late Quaternary Colorado river-delta evolution, *Basin Res.*, 13(3), 243–268.
- Wolman, M. G., and J. P. Miller (1960), Magnitude and frequency of forces in geomorphic processes, *J. Geol.*, 68, 54–74.
- Wood, L. J., F. G. Ethridge, and S. A. Schumm (1993), The effects of rate of base-level fluctuation on coastal-plain, shelf, and slope depositional systems: An experimental approach, *Spec. Publ. Int. Assoc. Sedimentol.*, 18, 43–54.

S. Fagherazzi, Department of Geological Sciences, Florida State University, Tallahassee, FL 32306-4120, USA. (sergio@csit.fsu.edu)

A. D. Howard and P. L. Wiberg, Department of Environmental Sciences, University of Virginia, P.O. Box 400123, Charlottesville, VA 22903, USA. (ah6p@virginia.edu; pw3c@virginia.edu)